



Spray-dried, Biodegradable, Linezolid-loaded Microspheres for Use in the Treatment of Lung Diseases

Mazen Gharsan Al-Gharsan^{a++*}

^a *Department of Pharmaceutical Sciences, College of Clinical Pharmacy, King Faisal University, Saudi Arabia.*

Author's contribution

The sole author designed, analysed, interpreted and prepared the manuscript.

Article Information

DOI: 10.9734/JAMPS/2023/v25i9642

Open Peer Review History:

This journal follows the Advanced Open Peer Review policy. Identity of the Reviewers, Editor(s) and additional Reviewers, peer review comments, different versions of the manuscript, comments of the editors, etc are available here: <https://www.sdiarticle5.com/review-history/107189>

Original Research Article

Received: 02/08/2023

Accepted: 04/10/2023

Published: 09/10/2023

ABSTRACT

Introduction: Researchers worldwide are currently seeking innovative treatment options to combat the alarming increase in bacterial resistance to antimicrobial drugs. Staphylococcus aureus, a frequently encountered and potentially life-threatening bacterium, has become particularly problematic. Linezolid is one of the few medicines on the market that can treat bacteria resistant to other antibiotics. This is the first antibacterial oxazolidinone that has shown to be therapeutically efficacious. Linezolid is a new Oxazolidinone medicine. It kills a broad spectrum of bacteria, including Staphylococcus aureus.

Objectives: To reduce non-target organ adverse effects associated with frequent and chronic Linezolid usage, we developed biodegradable, lung-targeted microspheres with sustained release profile.

Methods: In this work, a Buchi B-90 nanospray drier was used to prepare a Linezolid-loaded carbopol microsphere (CLSMO)-based formulation. The spray-drying process was optimized using a face-centered central composite design (CCD).

⁺⁺ Master degree of pharmaceutical science, Under the supervision of Professor Sri Harsha;

*Corresponding author: E-mail: Phmz2040@gmail.com;

Results: The average particle size was 7.516 μm , and the surface of the microspheres was shriveled, according to scanning electron microscope imaging. Drug content and yield were determined to be 73% \pm 3.1% and 72% \pm 2.4%, respectively, and drug release (99.1%) peaked for up to 12 hours in vitro. FTIR spectral analysis results suggest that there are no significant physical and chemical interactions between the functional groups of Linezolid and carbopol 934P polymer which ultimately form a stable blend. Linezolid, Carbopol, and CLSMO all had XRD patterns that showed the linezolid would be molecularly dispersed in the polymer. The DSC findings revealed the drug's amorphous nature, which explains the absence of characteristic peaks, indicating a lack of well-defined crystalline structure.

Conclusion: The optimized formulation shows significant potential for use as a drug-delivery system in in-vivo applications, particularly in targeted drug delivery to the lungs.

Keywords: Drug delivery; lung diseases; therapeutic utility.

1. INTRODUCTION

1.1 Introduction

Drug delivery is the process of delivering a medication or other pharmacologically active substance to a target cell in order to treat a condition or health problem [1,2]. Drug delivery can take place by oral or intravenous or rectal, intranasal, intramuscular, transdermal, subcutaneous, pulmonary, or buccal [3,4]. However, these methods have certain drawbacks, for example instability, side effects, uncontrolled release, slow absorption, and enzymatic degradation [5,6]. To address these issues, targeted drug delivery (TDD) has been developed.

Microspheres are used for delivery of drugs to a particular target site because of its properties as its size is tiny, its shape is spherical and it is biodegradable particles [7,8]. It offers enhanced drug loading capabilities and can be designed to provide specific release profiles and target specific tissue sites. Not only that but also it can be can be engineered to possess certain desirable characteristics like sustained or controlled release, improved drug solubility, and increased drug stability [9,10]. Drugs which are sensitive to temperature or PH or light and different types of drugs can be used with microspheres.

1.2 Research Aim and Objectives

The aim of this study is to develop and characterize microspheres containing linezolid for lung delivery, with the particle size ranging from 5-15 microns by intravenous route.

2. METHODOLOGY

2.1 Formulation Studies

Spray drying is a typical method for preparing microspheres for drug delivery applications[11]. It

has been used to manufacture a variety of drug delivery systems, like microspheres, nanocomposites, nanospheres, and liposomes. It is an easy, flexible, and affordable approach [4,12].

2.2 Optimization

There are some variables affect how well a product turns out after being spray-dried these variables may be critical process variables or formulation variables or both [12]. Thus, the transfer of this technology from the laboratory scale to the production plant is significantly speed up by using the quality by design (QbD) method in conjunction with process analytical technology (PAT). The relationships between them in such a procedure are complicated and occasionally challenging to predict because there are many parameters that may be manipulated [13].

Procedure: Carbopol microspheres containing linezolid were prepared using the Buchi Nano Spray Dryer technique with the carbopol concentration (100mg–500 mg), inlet temperature (80°C–100°C) and flow rate (20–25 mL/h). 1:1 solutions of carbopol and linezolid were prepared in 100 mL of water, warmed to 25°C, with a viscosity 15 cP (centipoise) suitable for spraying through the nozzle. The dispersion was then fed through a 7 mm nozzle and the outlet temperature was kept in the range of 30°C–50°C. All samples were filtered prior to spray drying in order to prevent nozzle blockage. The dried particles were collected manually with a particle scraper and stored in desiccators at room temperature for further examination.

2.3 Estimation of Pure Drug Linezolid

Estimation of linezolid in microspheres involves the preparation of a standard solution of linezolid

by dissolving an accurately weighed quantity of the drug in a methanol, then preparation of a series of dilutions by diluting the standard solution with the same solvent [10]. The absorbance of each solution is measured using an UV-visible spectrophotometer at a wavelength of λ_{max} of linezolid, which is 284 nm.

2.4 Percentage Recovery/ Yield

The percentage weight of the resulting microspheres was used to calculate the spray-dried small particle recovery [14]. which was compared to the initial amounts of carbopol and linezolid utilized in the formulation process, and this percentage can be calculated by the following equation

Equation 1: Microsphere recovery:

$$\text{Microspheres recovery} = \frac{\text{Recovered Weight of Microspheres}}{\text{Weight of the polymer used} + \text{Drug}} \times 100$$

2.5 Drug Loading in Microsphere

Drug loading is the amount of drug in a formulation, it is expressed as a percentage of the formulation's overall weight [15].

A solvent extraction approach was employed to determine the drug loading of linezolid in spray dried microspheres. At first the microspheres are homogenized in an acetonitrile solution. Then the filtrate is collected by filtration of the homogenized solution. The amount of drug in the filtrate is then measured using linezolid's UV spectrophotometry at 284 nm in wavelength. Finally, the drug loading is then determined by dividing the drug concentration in the filtrate by the sum of the microspheres' weight using the following equation.

Equation 2: drug loading:

$$\% \text{ Drug Loading} = \frac{\text{Quantity of Linezolid present}}{\text{Microspheres}} \times 100$$

2.6 Surface Morphology Procedure

The powders were imaged by a scanning electron microscope (SEM) run at an accelerating voltage of 10kV using Hitachi SU 3500. The powder in few μg were fixed on to stub by a double-sided sticky carbon tape and kept inside the SEM chamber and analyzed at different magnification like 60X, 200X, 500X.

1.10X and 2.50X respectively to obtain better clarity on the particle morphology/ topology.

2.7 Particle Size Measurement

The Particle Size distribution of a 10-milligram sample obtained from a spray dryer was determined using a Malvern Zetasizer Nano ZS (Malvern Instruments, Malvern, UK) [16]. The sample was suspended in 10 mL of an organic solvent and ultrasonicated, then added three-quarters full to a reusable glass cuvette. The distribution was measured by taking three readings and averaging the results.

2.8 Differential Scanning Calorimetry (DSC)

Differential Scanning Calorimetry (DSC) is a thermo analytical technique in which the difference in the amount of heat required to increase the temperature of a sample and reference are measured as a function of temperature. Both the sample and reference are maintained at nearly the same temperature throughout the experiment [17].

Procedure: DSC (Perkin-Elmer- 4000 series) experiments were carried out in order to characterize the physical state of the drugs. Samples of formulation were placed in aluminium pans and thermally sealed. The heating rate was 20°C per minute using nitrogen as the purge gas. The DSC instrument was calibrated for temperature using Indium. In addition, for enthalpy calibration Indium was sealed in aluminium pans with sealed empty pan as a reference.

2.9 X-ray Diffraction Analysis (XRD)

XRD analysis, is a technique used in materials science to study of the crystal structure, it is used to identify the crystalline phases present in a material and thereby reveal chemical composition information [18].

2.10 Fourier Transform Infrared Spectrometry (FTIR)

Procedure: Infrared spectra of samples were recorded in Bruker ATR alpha kept at an ambient temperature of $25.0 \pm 0.5^\circ\text{C}$. The analytical procedure was simple and did not need any special sample preparation [19]. The spectra were recorded by placing the samples on a zinc

selenoid crystal plate and screwing the anvil over the sample carefully and scanning. The samples in region of 4000-400 cm⁻¹ to determine various functional groups. The IR spectra of the samples was checked for any possible drug excipients interaction [20].

2.11 *In vitro* Release Studies

Release studies are key components in the development of conventional drug delivery systems and novel drug delivery formulations [21]. These studies are important in determining the optimal release rate of the drug from the delivery system, as well as its effectiveness in targeting the desired site of action.

Procedure: predetermined time intervals to measure the drug content which was determined at 252 nm using a UV-VIS spectrophotometer (1601; Shimadzu Corporation). The data obtained from the studies were analyzed using

Sigma plot software version 12.0.3.0 (Systat Software, Inc., San Jose, CA, USA) and different kinetic models were used to understand the release mechanism. The experiment was conducted in triplicate (mean \pm SD, n=3). The obtained data were fitted to different kinetic models to understand the release mechanism using Sigmaplot software version 14.5 (Systat Software, Inc., San Jose, CA, USA).

3. RESULTS AND DISCUSSION

3.1 Optimization

The results of particle size optimization were fitted to a quadratic regression model, resulting in the maximum values of R² and model sum of squares. Analysis of variance (ANOVA) was performed on the results, and showed that the model was statistically significant.

Table 1. Software and experimental design

| | | | |
|------------------------|-------------------|----------------|------------|
| File Version | 12.0.3.0 | | |
| Study Type | Response Surface | Subtype | Randomized |
| Design Type | Central Composite | Runs | 15 |
| Design Model | Quadratic | Blocks | No Blocks |
| Build Time (ms) | 5.00 | | |

Table 2. Experimental plan for linezolid microspheres

| Name | Units | Type | Low | High |
|----------------------|--------------|-------------|------------|-------------|
| Carbopol Conc | mg | Factor | 100 | 500 |
| Intel Temp | DC | Factor | 80 | 100 |
| Feed Flow | ml | Factor | 20 | 25 |
| Particle size | nm | Response | 5980 | 9004 |

Table 3. Experimental design layout

| Std | Run | Factor 1 | Factor 2 | Factor 3 | Response 1 |
|------------|------------|------------------------|---------------------|--------------------|----------------------|
| | | A:Carbopol Conc | B:Intel Temp | C:Feed Flow | Particle size |
| | | Mg | DC | ml | Nm |
| 15 | 1 | 300 | 90 | 23 | 7200 |
| 9 | 2 | 300 | 90 | 19 | 6400 |
| 11 | 3 | 300 | 90 | 23 | 7350 |
| 14 | 4 | 300 | 90 | 23 | 7125 |
| 12 | 5 | 300 | 90 | 23 | 7300 |
| 3 | 6 | 100 | 100 | 25 | 7130 |
| 4 | 7 | 100 | 80 | 20 | 6368 |
| 7 | 8 | 300 | 76 | 23 | 8875 |
| 13 | 9 | 300 | 90 | 23 | 7115 |
| 10 | 10 | 300 | 90 | 26 | 8315 |
| 5 | 11 | 17 | 90 | 23 | 5980 |
| 1 | 12 | 500 | 100 | 20 | 7884 |
| 8 | 13 | 300 | 104 | 23 | 6265 |
| 6 | 14 | 583 | 90 | 23 | 8395 |
| 2 | 15 | 500 | 80 | 25 | 9004 |

3.2 Experimental Design Methodology

An experimental design methodology was employed to prepare batches of linezolid, with the aim of obtaining a desired particle size range (between 5–15 μm) [22]. A rotatable central composite design was chosen to investigate the effects of three operating variables (concentration of polymer, feed flow rate, and rotation speed) on the particle size of the microspheres, and the results of the experiment were analyzed using the Stat-Ease software.

3.3 Estimation of Pure Drug Linezolid

After that a calibration curve is plotted as X-axis was the concentration of the standard solution, and Y-axis was the absorbance of the respective solution, this calibration curve is used to calculate the concentration of linezolid in the test solution. An aliquot of the test solution is taken and its absorbance is measured using the UV-visible spectrophotometer at the same wavelength of λ_{max} of linezolid and using the calibration curve, the concentration of linezolid in the test solution is determined.

3.4 Drug Loading and Yield

The particle yield for a CLSMO-1 formulation was computed to be $72\% \pm 2.4\%$. During the drying process, some of the product was found to bind to the electrostatic particle collector and electrodes, which was likely caused by the low density of the particles formed after drying. To reduce this issue, it is suggested to increase the

volume of liquid delivered into the drying chamber; however, some of the product will still be lost. The drug content of the same formulation was found to be $73\% \pm 3.1\%$.

The particle yield for a CLSMO-1 formulation was calculated to be $72\% \pm 2.4\%$. During the drying process, some of the particles was appeared to stick to the electrostatic particle collector and electrodes, which was most likely caused by the low density of the particles formed after drying. To address this issue, it is proposed that the volume of liquid fed into the drying chamber be increased [12]; however, some particles will still be lost. The drug content of the identical formulation was found to be $73\% \pm 3.1\%$.

3.5 Surface Morphology

There are three main reasons that make the importance of surface morphology studies for drug formulation. The first reason is: they provide information on the physical characteristics of a drug product. This information is essential for understanding the properties of the drug product, like its size, surface area, shape, porosity, and crystallinity. The second reason is: They can provide insight into the manufacturing process of a drug product, including particle size distribution and homogeneity which can help to optimize the manufacturing process and ensure that the drug product is of a consistent quality. The third reason is: They can help identify potential issues with a drug product, such as non-uniformity, particle agglomeration, or contamination which can be used to improve the quality of the drug product and reduce the risk of adverse events.

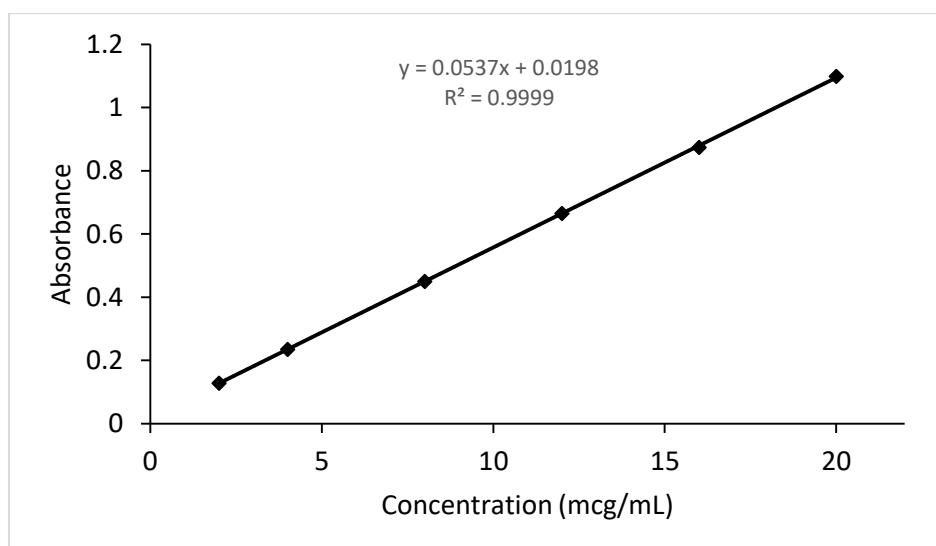


Fig. 1. Calibration curve of linezolid at 252nm

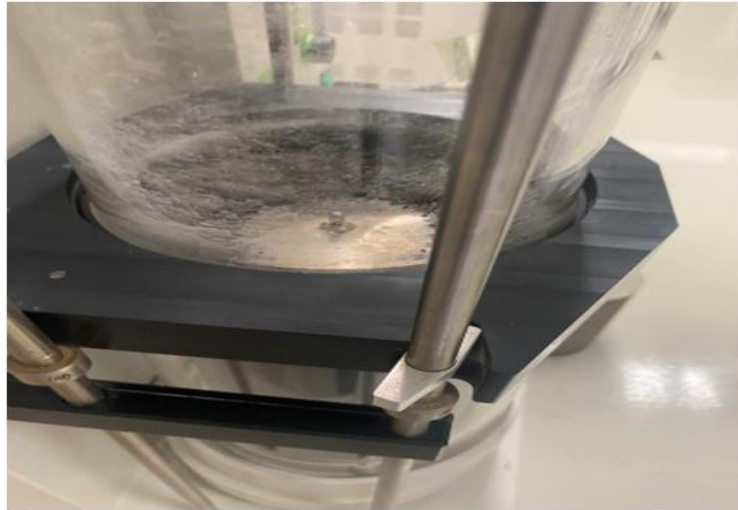


Fig. 2. Buchi Spray Dryer Glass Chamber showing particle sticking



Fig. 3. Buchi Spray Dryer Particle Collector showing particle sticking

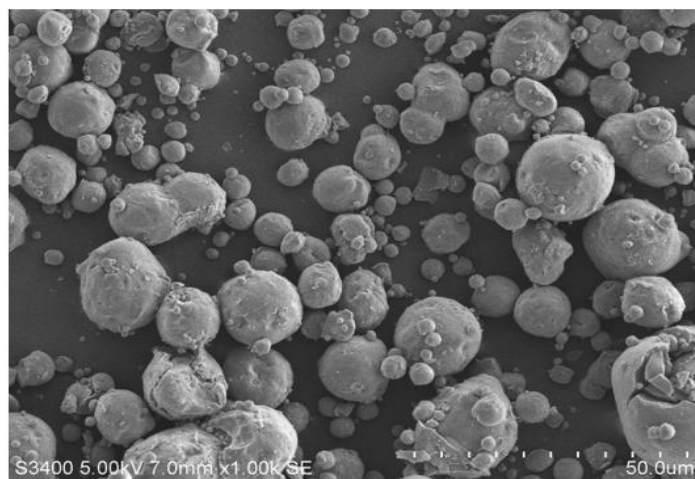


Fig. 4. Spray dried surface morphology of CLSMO-1

3.6 Particle Size Analysis

Particle size analysis is an important tool for optimizing targeted drug delivery to the lungs via the intravenous route by microspheres entrapped in the capillary network of the lungs. Particle size analysis can help to ensure that drugs are delivered to the lungs in an effective and safe manner by providing detailed information on the size and shape of the particles, as well as the efficiency of the delivery system.

The particle size of Carbopol microspheres containing linezolid was observed to be a key parameter for drug delivery. This particle size is in the optimal range of 5 - 15 μm , which is necessary for particle entering the lung tissue. Particle size also plays a significant role in targeting the particles to a specific region of the lung. The experimental data point showed a particle size of 7.302 μm , which is suitable for lung targeting.

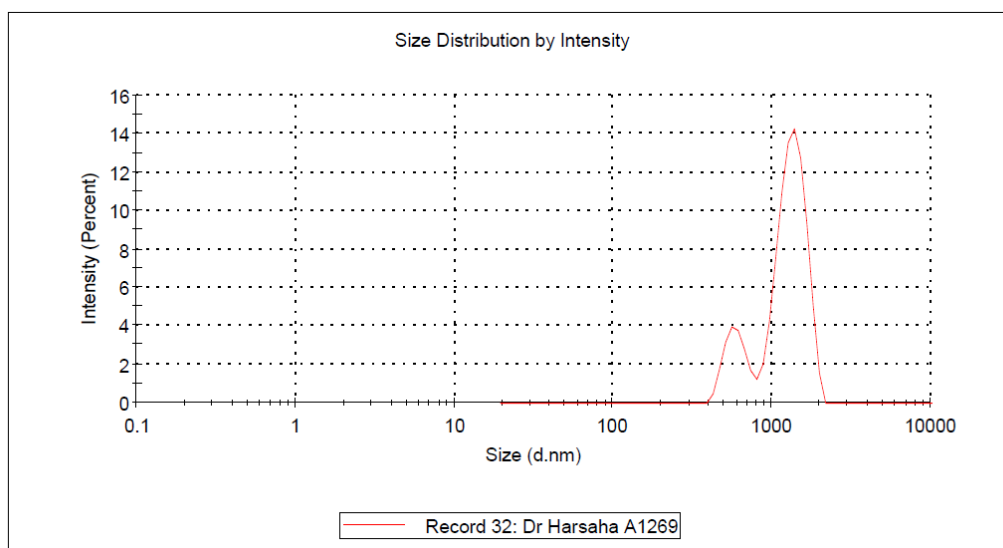


Fig. 5. Particle size analysis of Carbopol microspheres containing linezolid

Table 4. Results of experimental design table for three factors

| Std | Run | Factor 1 A: Carbopol Conc mg | Factor 2 B: Intel Temp DC | Factor 3 C: Feed Flow MI | Response 1 Particle size Nm |
|-----|-----|------------------------------------|---------------------------------|--------------------------------|-----------------------------------|
| 15 | 1 | 300 | 90 | 23 | 7200 |
| 9 | 2 | 300 | 90 | 19 | 6400 |
| 11 | 3 | 300 | 90 | 23 | 7350 |
| 14 | 4 | 300 | 90 | 23 | 7125 |
| 12 | 5 | 300 | 90 | 23 | 7300 |
| 3 | 6 | 100 | 100 | 25 | 7130 |
| 4 | 7 | 100 | 80 | 20 | 6368 |
| 7 | 8 | 300 | 76 | 23 | 8875 |
| 13 | 9 | 300 | 90 | 23 | 7115 |
| 10 | 10 | 300 | 90 | 26 | 8315 |
| 5 | 11 | 17 | 90 | 23 | 5980 |
| 1 | 12 | 500 | 100 | 20 | 7884 |
| 8 | 13 | 300 | 104 | 23 | 6265 |
| 6 | 14 | 583 | 90 | 23 | 8395 |
| 2 | 15 | 500 | 80 | 25 | 9004 |

Response 1: Particle size:

Table 5. ANOVA for Quadratic model

| Source | Sum of Squares | df | Mean Square | F-value | p-value | |
|------------------|----------------|----|-------------|---------|----------|-----------------|
| Model | 1.238E+07 | 9 | 1.376E+06 | 90.28 | < 0.0001 | significant |
| A-Carbopol Conc | 2.916E+06 | 1 | 2.916E+06 | 191.40 | < 0.0001 | |
| B-Intel Temp | 3.406E+06 | 1 | 3.406E+06 | 223.55 | < 0.0001 | |
| C-Feed Flow | 1.834E+06 | 1 | 1.834E+06 | 120.35 | 0.0001 | |
| AB | 85329.72 | 1 | 85329.72 | 5.60 | 0.0642 | |
| AC | 1.389E+06 | 1 | 1.389E+06 | 91.15 | 0.0002 | |
| BC | 80.17 | 1 | 80.17 | 0.0053 | 0.9450 | |
| A ² | 4123.68 | 1 | 4123.68 | 0.2707 | 0.6251 | |
| B ² | 3.545E+05 | 1 | 3.545E+05 | 23.27 | 0.0048 | |
| C ² | 90180.11 | 1 | 90180.11 | 5.92 | 0.0592 | |
| Residual | 76180.37 | 5 | 15236.07 | | | |
| Lack of Fit | 32450.37 | 1 | 32450.37 | 2.97 | 0.1600 | not significant |
| Pure Error | 43730.00 | 4 | 10932.50 | | | |
| Cor Total | 1.246E+07 | 14 | | | | |

Factor coding is **Coded**.

Sum of squares is **Type III – Partial**

The Model F-value of 90.28 implies the model is significant. There is only a 0.01% chance that an F-value this large could occur due to noise.

P-values less than 0.0500 indicate model terms are significant. In this case A, B, C, AC, B² are significant model terms. Values greater than 0.1000 indicate the model terms are not significant. If there are many insignificant model terms (not counting those required to support hierarchy), model reduction may improve the model.

The Lack of Fit F-value of 2.97 implies the Lack of Fit is not significant relative to the pure error. There is a 16.00% chance that a Lack of Fit F-value this large could occur due to noise. Non-significant lack of fit is good -- we want the model to fit.

The Predicted R² of 0.7131 is not as close to **the Adjusted R²** of 0.9829 as one might normally expect; i.e., the difference is more than

0.2. This may indicate a large block effect or a possible problem with the model and/or data. Things to consider are model reduction, response transformation, outliers, etc. All empirical models should be tested by doing confirmation runs.

Adeq Precision measures the signal to noise ratio. A ratio greater than 4 is desirable. The ratio of 28.917 indicates an adequate signal. This model can be used to navigate the design space.

The equation in terms of actual factors can be used to make predictions about the response for given levels of each factor. Here, the levels should be specified in the original units for each factor. This equation should not be used to determine the relative impact of each factor because the coefficients are scaled to accommodate the units of each factor and the intercept is not at the center of the design space.

The linear pattern observed in the predicted vs. actual values of particle size shows that the observed responses were in good correlation with the predicted one.

Table 6. Fit statistics

| | | | |
|------------------|---------------|--------------------------------|---------------|
| Std. Dev. | 123.43 | R² | 0.9939 |
| Mean | 7380.40 | Adjusted R² | 0.9829 |
| C.V. % | 1.67 | Predicted R² | 0.7131 |
| | | Adeq Precision | 28.9170 |

Table 7. Final equation in terms of actual factors

| Particle size | = |
|---------------|----------------------------|
| +26352.70602 | |
| +32.12473 | Carbopol Conc |
| -514.82561 | Intel Temp |
| -30.47334 | Feed Flow |
| +0.103277 | Carbopol Conc * Intel Temp |
| -1.66655 | Carbopol Conc * Feed Flow |
| +0.253258 | Intel Temp * Feed Flow |
| +0.000578 | Carbopol Conc ² |
| +2.14370 | Intel Temp ² |
| +17.29926 | Feed Flow ² |

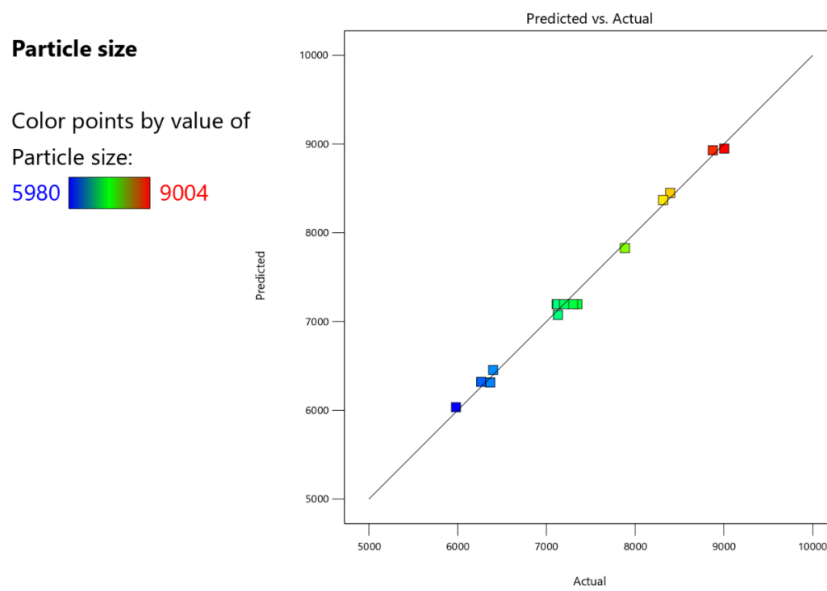


Fig. 6. Predicted vs. Actual

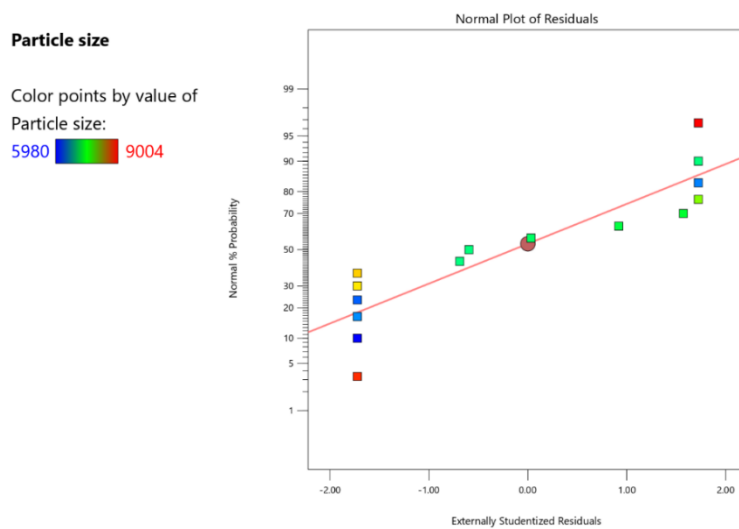


Fig. 7. Normal plot

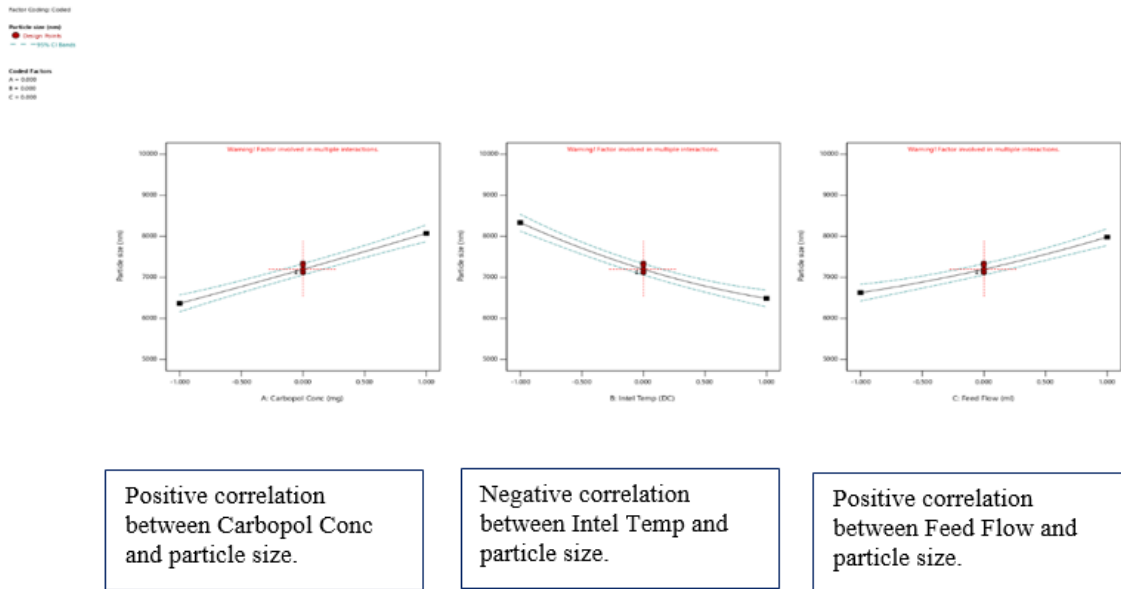


Fig. 8. Factors effects

The normal probability plot of the residuals suggests that the error terms are normally distributed.

From the previous figure there are: Positive correlation between particle size and both Carbopol Conc and Feed Flow, but negative correlation between Intel Temp and particle size.

3.7 Interpretation

From the previous figure it is noticed when the Carbopol Conc reached 500mg, big size particles were observed with temperature between 80°C

to 85°C. As temperature increases in spray-drying preparation, the size of the particles decreases.

From the previous figure it is noticed when the Carbopol Conc increases from 100mg towards 500mg with an increase in feed flow from minimum to maximum, increase in particles was observed.

Analyzing the 2D contour plot of the effects of interaction on the particle size, big size of particles was observed when feed flow reached at highest 25ml with temperature in the range of 80°C to 85°C.

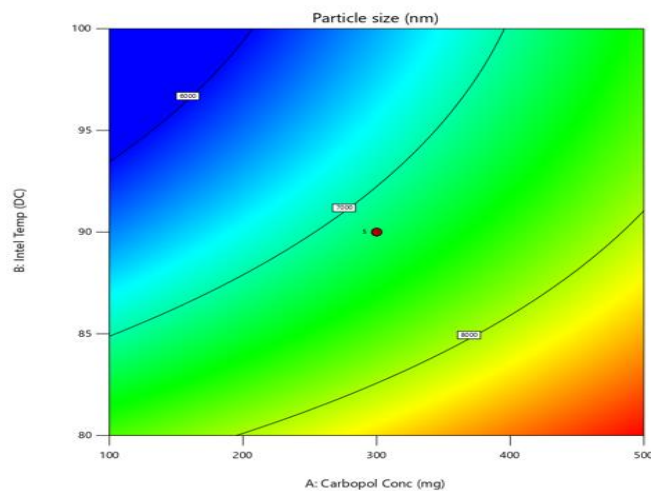


Fig. 9. Contour Plots (2D) particle size, intel temp., and Carbopol conc.

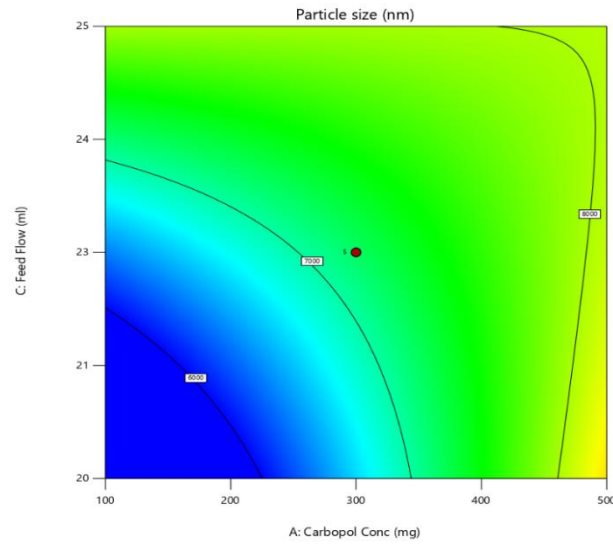


Fig. 10. Contour Plots (2D) particle size, feed flow, and Carbopol conc

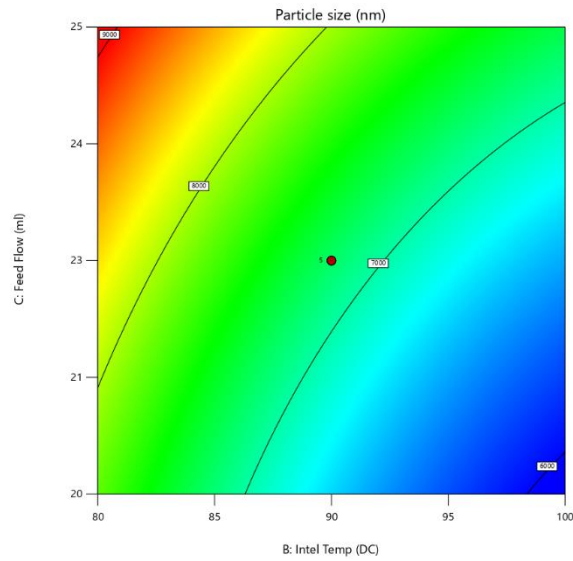


Fig. 11. Contour Plots (2D) particle size, feed flow, and intel Temp

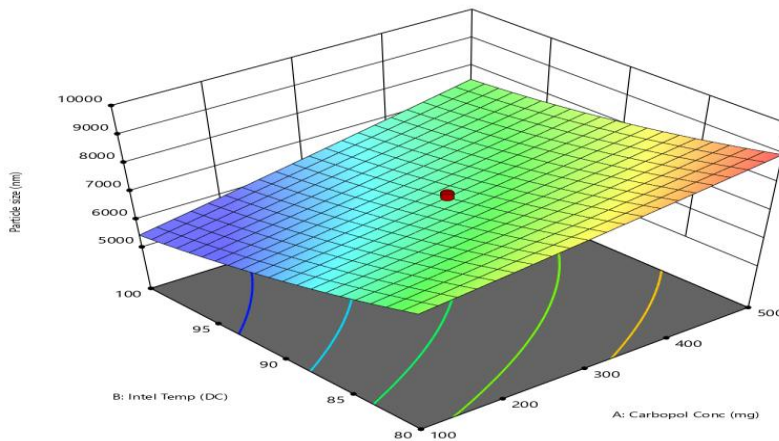


Fig. 12. Contour Plots (3D) particle size, intel temp., and Carbopol conc

3.8 Interpretation: (Effect of Carbopol conc on Particle Size)

The interaction of the Carbopol Conc with the particle size is significant. It is observed that increasing the concentration of Carbopol results in increasing in size of the particles, this is due to more solid in a droplet may increase the size and

also the droplet contains lesser amount to vaporize.

3.9 Interpretation: (Effect of Feed Flow on Particle Size)

The interaction of the Feed Flow with the particle size is significant. It is observed that with an increase in flow rate, increase in particle size.

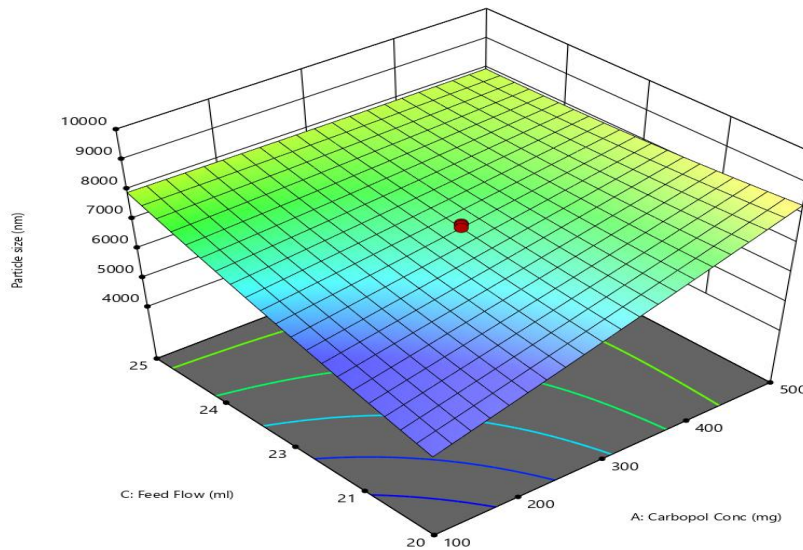


Fig. 13. Contour Plots (3D) particle size, feed flow, and Carbopol conc

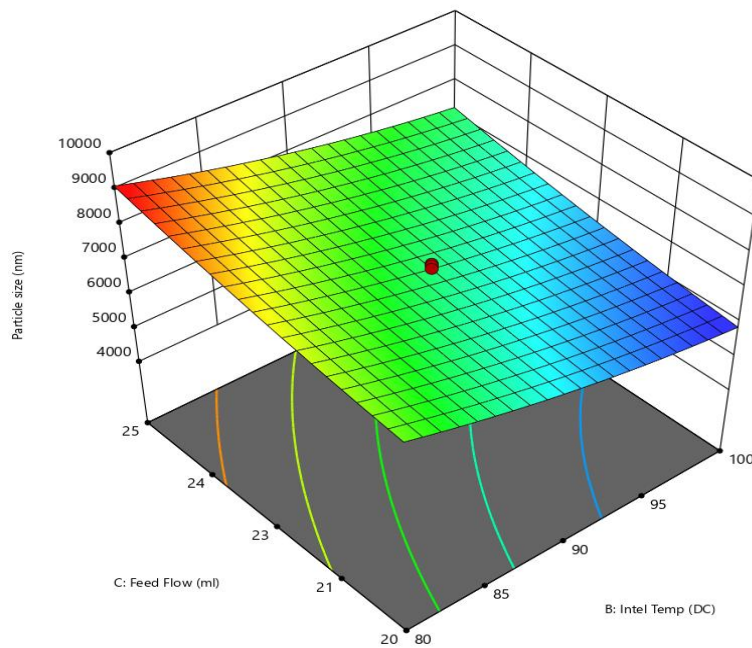


Fig. 14. Contour Plots (3D) particle size, feed flow, and intel Temp

3.10 Interpretation: (Effect of Intel Temp on Particle Size)

The interaction of the feed flow and particle size is significant. Surprisingly, an increase in inlet temperature shows a decrease in particle size.

The Anova table for quadratic model shows, all three factors intel temp, carbopol conc. and feed flow are statistically significant for particle size (P-value<0.05). All three factors affect the size of particles in spray drying process. It is observed that particle size increases with feed flow and carbopol conc. also increases while intel temperature decreases.

3.11 Starting Points

From the previous table there three starting points with three formulation codes. The first at Carbopol Conc. 300, intel Temp. 90, feed flow 23, predicted particle size 7322 and actual particle size μm 7.302 and its code is CLSMO-1, the second at Carbopol Conc. 105, intel Temp. 83, feed flow 23, predicted particle size 7524 and

actual particle size μm 7.516 and its code is CLSMO-2, the last at Carbopol Conc. 166, intel Temp. 80, feed flow 21, predicted particle size 7544 and actual particle size μm 7.552 and its code is CLSMO-3.

The results of the number optimization solution showed that three formulations were selected for further evaluation. The response for particle size was found to be similar to the response predicted by the design expert software. Following this, further studies were conducted using the best selected formulation code from the table.

3.12 Differential Scanning Calorimetry

The results obtained from the differential scanning calorimetry (DSC) analysis provided valuable insights into the thermal properties of the Linezolid, Carbopol, and CLSMO formulation. Importantly, no noticeable shift or alteration in the melting point was observed. This finding suggests that the presence of Carbopol and the encapsulation of Linezolid within the microspheres did not significantly affect the thermal behavior of the drug.

Table 8. Number of Starting Points: 105

| Carbopol Conc | Intel Temp | Feed Flow | Predicted Particle Size | Actual Particle Size μm | Formulation Code |
|---------------|------------|-----------|-------------------------|------------------------------------|------------------|
| 300 | 90 | 23 | 7322 | 7.302 | CLSMO-1 |
| 105 | 83 | 23 | 7524 | 7.516 | CLSMO-2 |
| 166 | 80 | 21 | 7544 | 7.552 | CLSMO-3 |

CLSMO – Carbopol, linezolid, Microspheres, Spray Drying

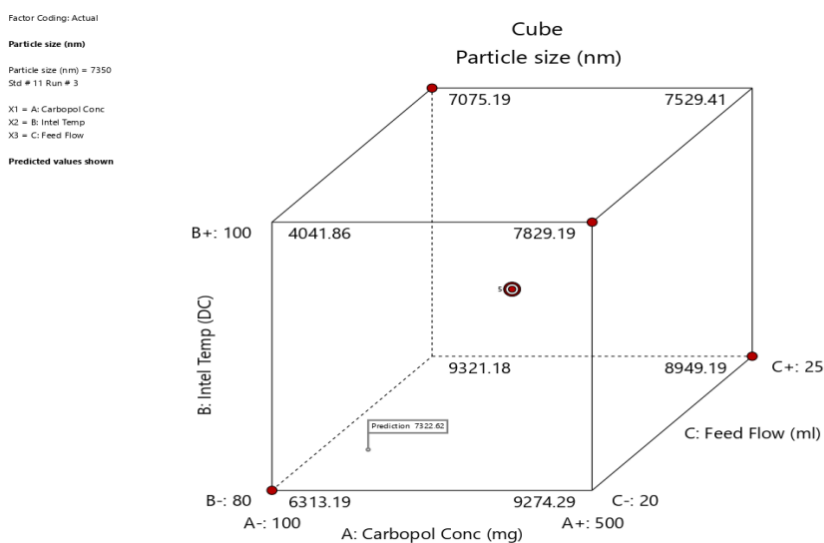


Fig. 15. Particle size in CLSMO-1 (a)

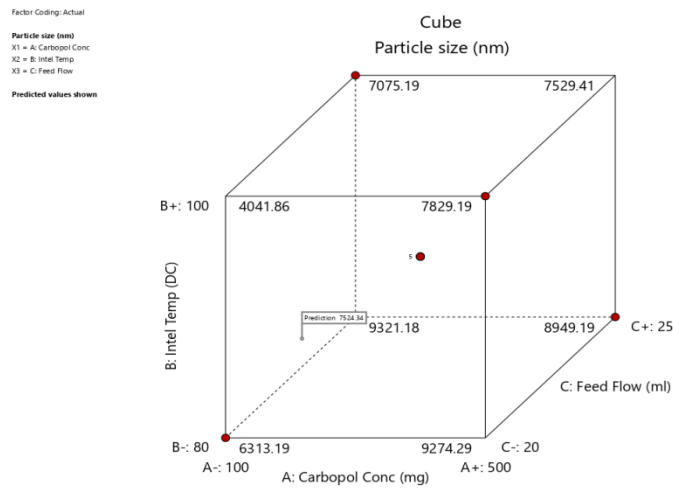


Fig. 16. Particle size in CLSMO-1 (b)

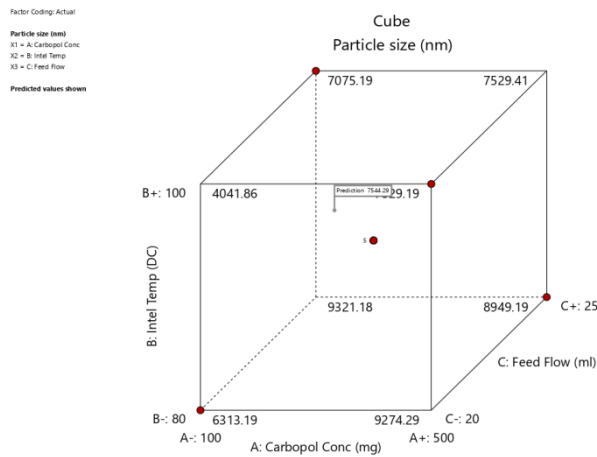


Fig. 17. Particle size in CLSMO-1 (c)

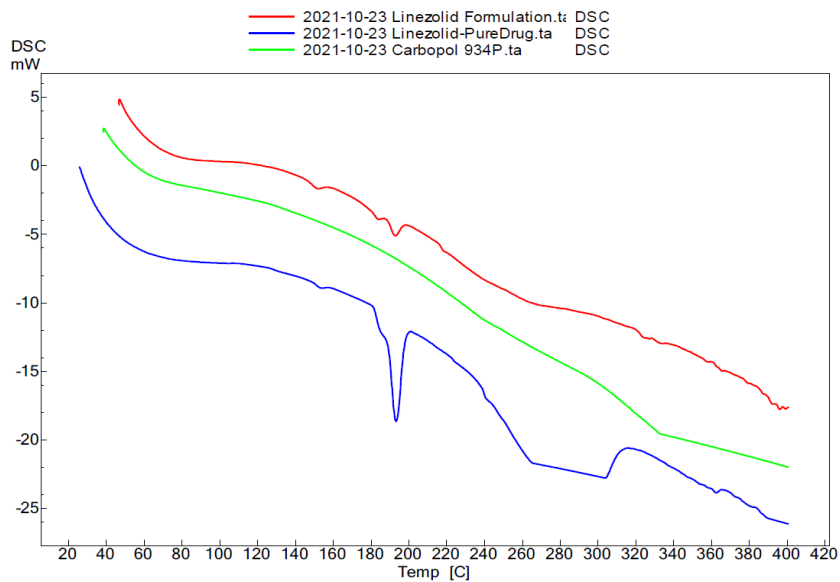


Fig. 18. DSC of linezolid formulation, linezolid pure drug, and Carbopol

3.13 XRD Studies

XRD analysis, way of the study of the crystal structure, is used to identify the crystalline phases present in a material and thereby reveal chemical composition information. Identification of phases is achieved by comparison of the acquired data to that in reference databases. In XRD analysis, a focused X-Ray beam is shot at the sample at a specific angle of incidence. The X-Rays deflect or "diffract" in various ways depending on the crystal structure (inter-atomic distances) of the sample. The locations (angles) and intensities of the diffracted X-Rays are measured.

X-ray diffraction analysis (XRD) is a technique used in materials science to determine the crystallographic structure of a material. XRD works by irradiating a material with incident X-rays and then measuring the intensities and scattering angles of the X-rays that leave the material.

Present investigation of XRD studies qualitatively revealed the physical state and compatibility of the drug Linezolidin in the microsphere (MS) of Carbopol 934. In our investigation we chose two

characteristics peaks at 2 Theta angles (14.40 and 22.12) observed in the XRD pattern of the pure Linezolidin were compared with its formulation in microsphere of Carbopol 934P.

The characteristics peaks of both the pure Linezolidin and its formulation in microsphere of Carbopol 934P were found to show similar XRD patterns but with different in their intensities as shown in the following figure.

Both XRD pattern of pure Linezolidin and formulation in microsphere are characterized by the interplanar d-spacing, the intensities height (H) and area under the curve the peaks in the pattern as shown in the following tables.

The relative intensities heights of the characteristics peaks of our microsphere formulation were less than those of pure Linezolidin. It is cleared from results that there is a decrease in the crystalline peaks of Linezolidin in microsphere with increasing lattice spacing indicating that the drug has relatively become amorphous due to its dispersion in the amorphous region of semi crystalline polymeric microsphere of CLSMO at the molecular level.

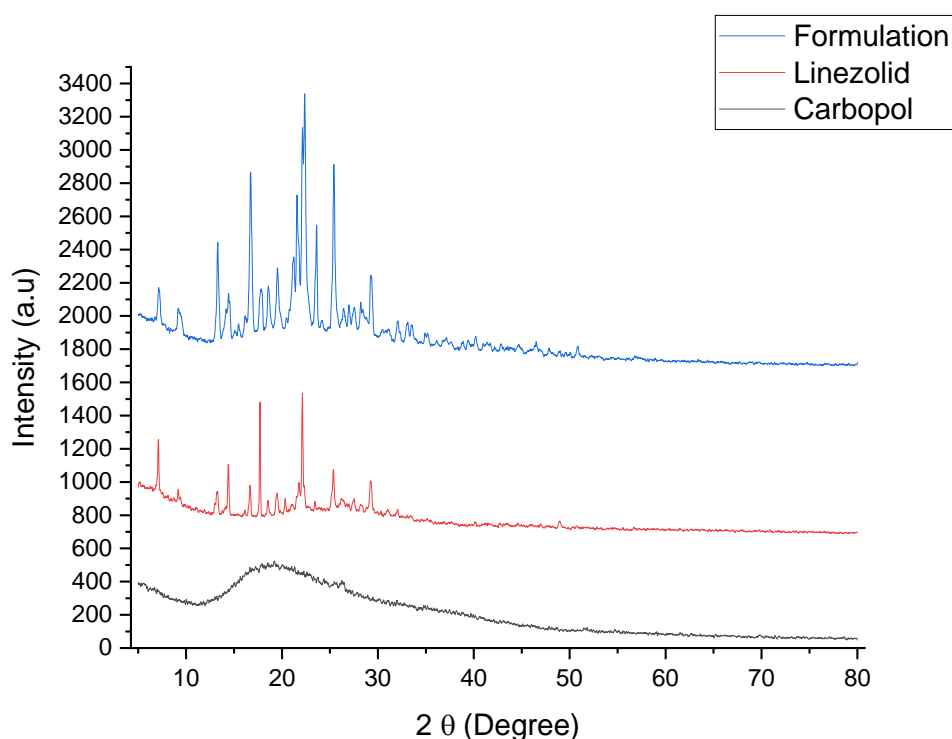


Fig. 19. XRD pattern of linezolid formulation, linezolid pure drug, and Carbopol

Table 9. 2 Theta, Lattice spacing (Å), Intensities (H) and Area under the curve the peaks in the Diffractogram of Linezolidin

| Linezolid | | | |
|-----------|---------------|----------------------|---------------------|
| 2 Theta | Intensity (H) | Area under the curve | Lattice spacing (Å) |
| 14.40749 | 275.38237 | 40.72298 | 6.15 |
| 22.12642 | 649.55377 | 120.49009 | 4.02 |

Table 10. 2 Theta, Lattice spacing (Å), Intensities (H) and Area under the curve the peaks in the Diffractogram of Linezolidin formulation in microsphere

| Formulation in MS of Carbopol | | | |
|-------------------------------|---------------|----------------------|---------------------|
| 2 Theta | Intensity (H) | Area under the curve | Lattice spacing (Å) |
| 14.422 | 155.32681 | 47.81774 | 6.14 |
| 21.53483 | 486.83949 | 450.16384 | 4.13 |

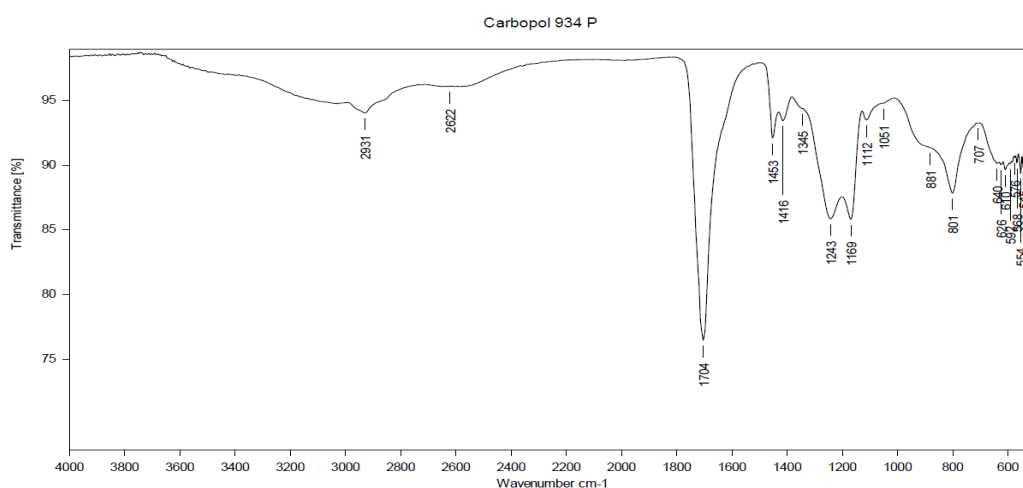


Fig. 20. FTIR of carbopol 934P

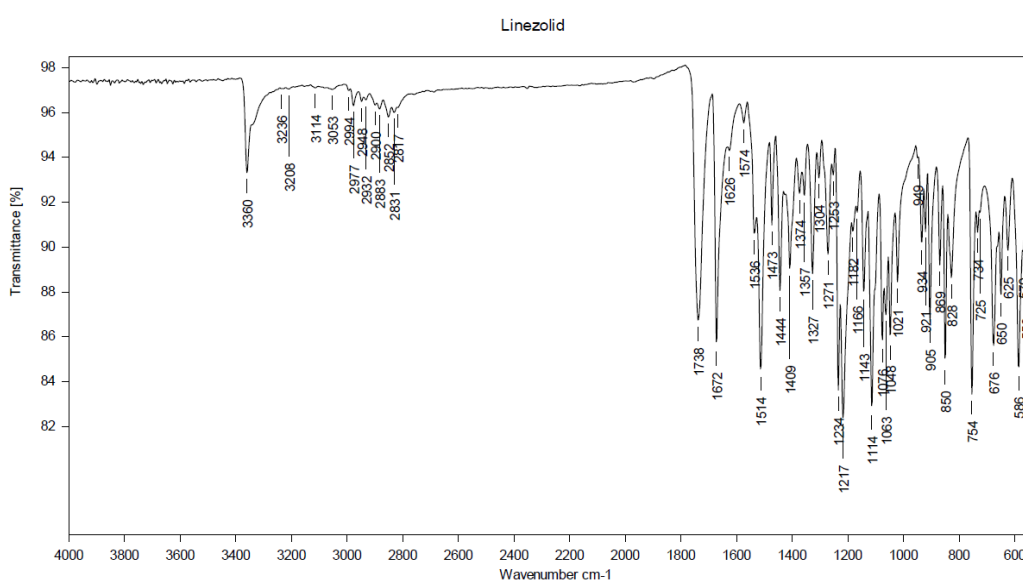


Fig.21. FTIR of Linezolid

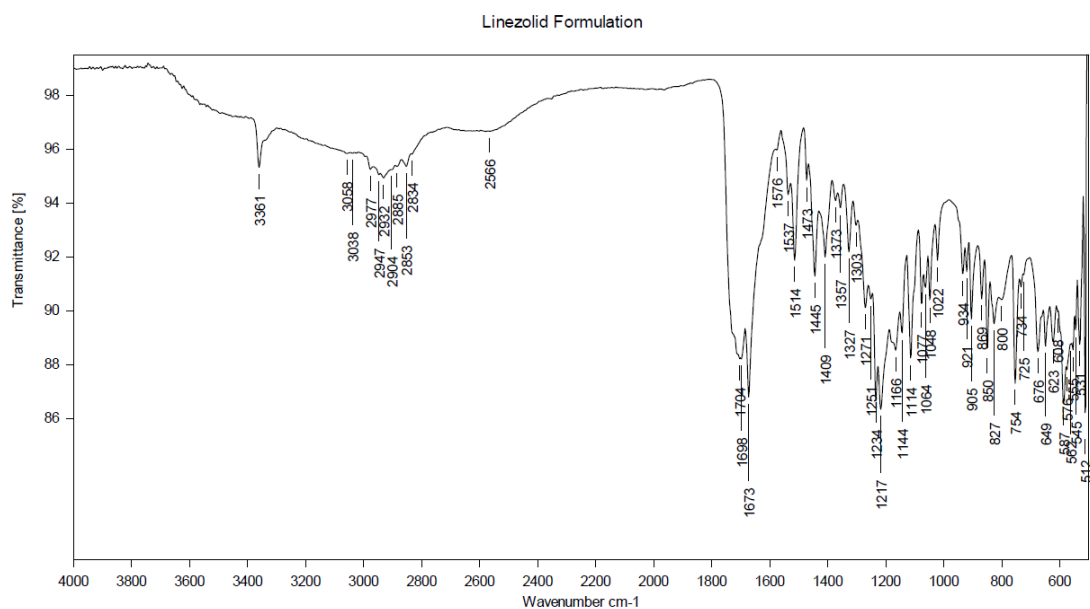
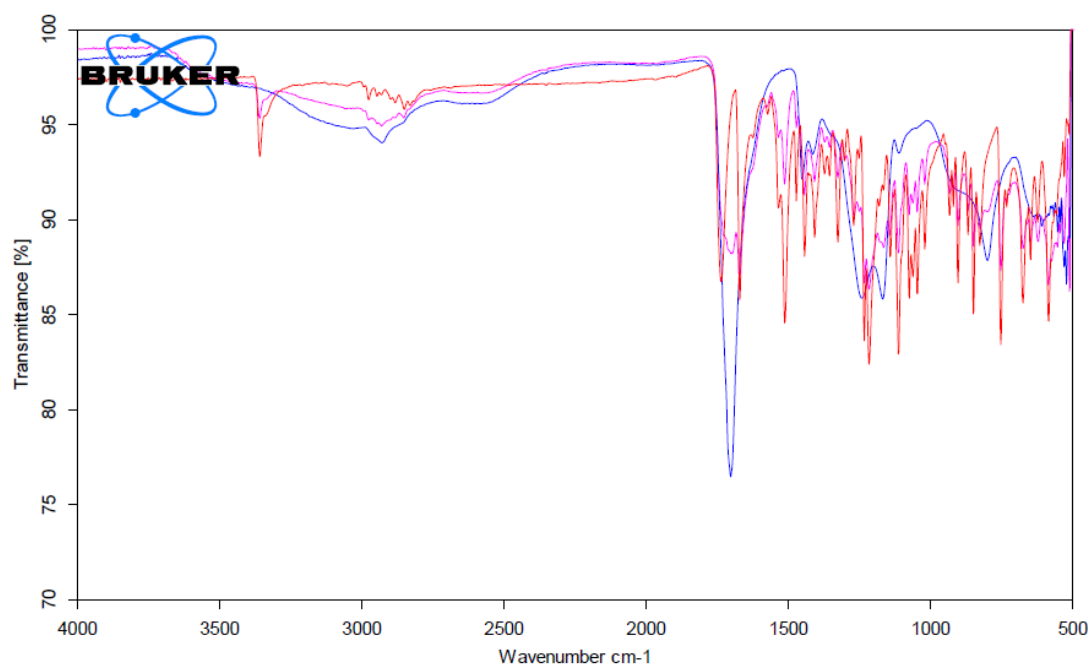


Fig. 22. FTIR of Linezolid formulation



| | | | |
|--------------------------------|-----------------------|-------|------------|
| C:\PRL\Linezolid.0 | Linezolid | Solid | 10/19/2021 |
| C:\PRL\Carbopol 934 P.0 | Carbopol 934 P | Solid | 10/19/2021 |
| C:\PRL\Linezolid Formulation.0 | Linezolid Formulation | Solid | 10/19/2021 |

Fig. 23. FTIR of Linezolid formulation

3.14 Fourier-Transform Infra-Red (FT-IR)

Results: The FTIR spectral analysis of any drug molecule gives insight of the functional groups

which can interact with drug carrier polymers and causes a shift in frequency and bandwidth of absorption peaks. Therefore, FTIR spectroscopy is one of important tools to find out the

interactions and compatibility between the drug and polymers. The present investigation was carried out to prepare microspheres drug delivery system using linezolid antibiotic drug and carbopol 934p polymer.

Linezolid consists of 1, 3-oxazolidin-2-one bearing an N-3-fluoro-4-(morpholin-4-yl) phenyl group as well as an acetamidomethyl group at position 5. The IR spectra of linezolid along with the physical mixture of linezolid with carbopol 934p polymer are shown in the previous figures which displayed many intense, sharp absorption peaks that are due to the different functional groups present in the molecules. In the IR spectra of linezolid the wave number at 3360cm^{-1} and at 1672cm^{-1} showed the N-H stretching and N-H bending respectively. The wave number from 2817cm^{-1} to 2994cm^{-1} disclosed the presence C-H stretching and 1114cm^{-1} showed the ether functional group in morpholine moiety. The wave numbers of 1738cm^{-1} and 1672cm^{-1} are the characteristics absorption peaks which showed the presence of C=O stretching of an oxazolidinone carbonyl and C=O stretching of an

acetamide carbonyl. The wave number at 1574cm^{-1} indicated the presence of C=C aromatic and the wave number 1409cm^{-1} corresponded the C-H scissoring & bending. The characteristics peaks of pure Linezolid at 3360 , 1672 , 2817 to 2994 , 1114 , 1738 and 1672cm^{-1} were also reported by other researcher in their study which is almost similar to peaks found in our study. Thus, indicating the identity and purity of the Linezolid drug. In IR spectra of carbopol 934p polymer has been presented. The recorded bands were found at 1704 , 1169 and 1112cm^{-1} wavenumbers due to the presence of carbonyl group. It has been observed in this analysis that Linezolid within microspheres of carbopol, drug-polymer physical mixture, contained the same peaks and preserved its individual peaks at the same wavenumbers as in its own spectrum. Similarly, no change in position of spectral peaks of carbopol polymer were observed before and after formulation. This investigation results suggest that there are no significant physical and chemical interactions between the functional groups of Linezolid and carbopol 934P polymer which ultimately form a stable blend.

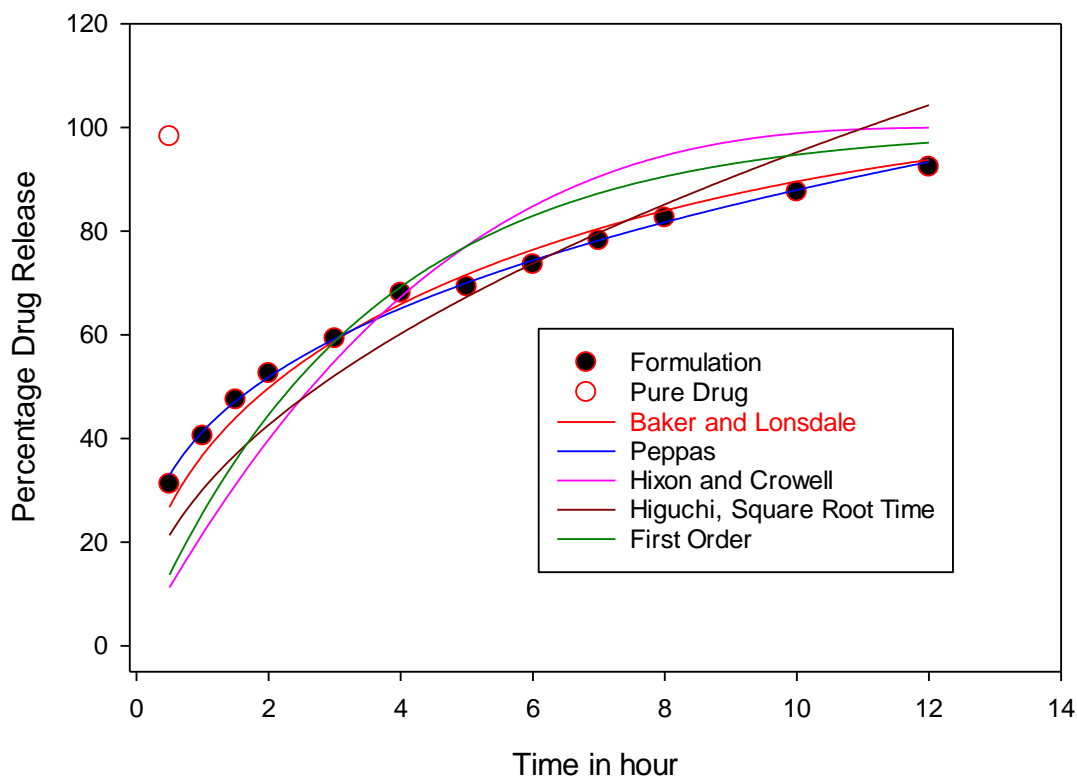


Fig. 24. *In vitro* release kinetics

3.15 *In vitro* Release Kinetics

As shown in the above figure the pure drug released 100% in first hour and at the same time CLSMO drug released 30%. The efficacy of linezolid-containing Carbopol microspheres in drug delivery has been studied extensively. It has been found that the linezolid released 95.4% of the drug within the first half hour, while 22.11% of linezolid-containing Carbopol microspheres is released in the first half hour and the remaining drug is released completely (99.1%) within 12 hrs. This drug-release pattern demonstrated an initial burst and is consistent with a biphasic model due to the loosely embedded drug on the particle surface. In the case of acute bacterial infections, the loading dose of 4–6 $\mu\text{g kg}^{-1}$ of linezolid is given intravenously over a 10-min period. Clinically, the initial burst release is important, as it acts as a loading dose, which helps to reach the minimum therapeutic concentration in the blood to show the drug's action. The release mechanism is studied by fitting the data to various kinetic models (SigmaPlot Ver 14.5) to understand the release mechanism, such as Baker and Lonsdale ($r^2=0.9789$), Peppas ($r^2=0.9960$), Hixon and Crowell ($r^2=0.5391$), Higuchi ($r^2=0.8175$), and First Order ($r^2=0.7300$). The regression square value of each of the five *in vitro* release kinetics - Baker and Lonsdale, Peppas, Hixon and Crowell, Higuchi, and First Order. The regression square value is a measure of how well the data fits the model, and a higher value indicates a better fit. The Peppas model had the highest regression square value of 0.9789.

The Baker and Lonsdale model had the highest regression square value of 0.9789, indicating that it had the best fit to the data. The Peppas model had a regression square value of 9960, indicating a very good fit. The Hixon and Crowell model had a regression square value of 5391, indicating a moderate fit. The Higuchi, Square Root model had a regression square value of 8175, indicating a good fit. Lastly, the First Order model had a regression square value of 0.7300, indicating a poor fit. The Peppas model assumes that the release of drug from a formulation is affected by the dissolution of the drug particles in a liquid medium. These findings are useful for the development of drug delivery systems for linezolid and other drugs.

4. CONCLUSION

In conclusion, the growing bacterial resistance to antimicrobial drugs has prompted researchers to

explore novel treatment options. *Staphylococcus aureus*, a commonly encountered and potentially fatal bacteria, poses a significant challenge due to its resistance to many antibiotics. Linezolid, as the first therapeutically efficacious antibacterial oxazolidinone, has shown promise in combating drug-resistant bacteria, including *Staphylococcus aureus*. However, the frequent and chronic use of Linezolid can lead to adverse effects on non-target organs.

The development of Linezolid-loaded carbopol microspheres (CLSMO) is a significant achievement in delivering drugs to targeted areas of the body. The observed characteristics, such as the shrivelled surface and average particle size, indicate the successful formation of the microspheres. Additionally, the absence of significant physical and chemical interactions between Linezolid and the carbopol 934P polymer, as revealed by FTIR spectral analysis, ensures the stability of the formulation. Overall, the optimized formulation of Linezolid-loaded microspheres holds promise as an effective drug-delivery system, particularly for targeted delivery to the lungs. This innovation has the potential to mitigate the adverse effects associated with prolonged Linezolid usage, ultimately improving treatment outcomes. Future *in vivo* applications of this formulation may revolutionize the field of targeted drug delivery and contribute significantly to combating bacterial infections, thereby addressing the global challenge of antimicrobial resistance.

CONSENT AND ETHICAL APPROVAL

It is not applicable.

COMPETING INTERESTS

Author has declared that no competing interests exist.

REFERENCES

1. Ferkol T, Schraufnagel D. The global burden of respiratory disease. *Annals of the American Thoracic Society*. 2014; 11(3):404-6.
2. Whitehead L, Seaton P. The effectiveness of self-management mobile phone and tablet apps in long-term condition management: a systematic review. *Journal of medical Internet research*. 2016; 18(5):e97.

3. Ramaiah B, Nagaraja SH, Kapanigowda UG, Boggarapu PR, Subramanian R. High azithromycin concentration in lungs by way of bovine serum albumin microspheres as targeted drug delivery: lung targeting efficiency in albino mice. *DARU Journal of Pharmaceutical Sciences*. 2016;24: 1-11.
4. Mahar R, Chakraborty A, Nainwal N, Bahuguna R, Sajwan M, Jakhmola V. Application of PLGA as a biodegradable and biocompatible polymer for pulmonary delivery of drugs. *AAPS PharmSciTech*. 2023;24(1):39.
5. James SS, Bednarz B, Benedict S, Buchsbaum JC, Dewaraja Y, Frey E, et al. Current status of radiopharmaceutical therapy. *International Journal of Radiation Oncology* Biology* Physics*. 2021;109(4): 891-901.
6. Hari SK, Gauba A, Shrivastava N, Tripathi RM, Jain SK, Pandey AK. Polymeric micelles and cancer therapy: An ingenious multimodal tumor-targeted drug delivery system. *Drug Delivery and Translational Research*. 2023;13(1): 135-63.
7. Orowitz TE, Ana Sombo PPAA, Rahayu D, Hasanah AN. Microsphere polymers in molecular imprinting: Current and future perspectives. *Molecules*. 2020;25(14): 3256.
8. Kocks JW, Chrystyn H, Van Der Palen J, Thomas M, Yates L, Landis SH, et al. Systematic review of association between critical errors in inhalation and health outcomes in asthma and COPD. *NPJ primary care respiratory medicine*. 2018; 28(1):43.
9. Verma NK, Alam G, Vishwakarma D, Mishra J, Khan WU, Singh AP, et al. Recent Advances in Microspheres Technology for Drug Delivery. *International Journal of Pharmaceutical Sciences and Nanotechnology (IJPSN)*. 2015;8(2):2799-813.
10. Wassif RK, Elkheshen SA, Shamma RN, Amer MS, Elhelw R, El-Kayal M. Injectable systems of chitosan in situ forming composite gel incorporating linezolid-loaded biodegradable nanoparticles for long-term treatment of bone infections. *Drug Delivery and Translational Research*. 2023:1-23.
11. Harsha NS. In vitro and in vivo evaluation of nanoparticles prepared by nano spray drying for stomach mucoadhesive drug delivery. *Drying Technology*. 2015;33(10): 1199-209.
12. SreeHarsha N, Venugopala KN, Nair AB, Roopashree TS, Attimarad M, Hiremath JG, et al. An efficient, lung-targeted, drug-delivery system to treat asthma via microparticles. *Drug design, development and therapy*. 2019: 4389-403.
13. Gurung BD, Kakar S. An overview on microspheres. *Int J Health Clin Res*. 2020; 3(1):11-24.
14. Cerón A, Costa S, Imbernon R, de Queiroz R, de Castro J, Ferraz H, et al. Study of stability, kinetic parameters and release of lysozyme immobilized on chitosan microspheres by crosslinking and covalent attachment for cotton fabric functionalization. *Process Biochemistry*. 2023;128:116-25.
15. Rahmani F, Naderpour S, Nejad BG, Rahimzadegan M, Ebrahimi ZN, Kamali H, et al. The recent insight in the release of anticancer drug loaded into PLGA microspheres. *Medical Oncology*. 2023; 40(8):229.
16. Bagheri G, Schlenczek O, Turco L, Thiede B, Stieger K, Kosub JM, et al. Size, concentration, and origin of human exhaled particles and their dependence on human factors with implications on infection transmission. *Journal of Aerosol Science*. 2023;168:106102.
17. Zhang Z, He X, Zeng C, Li Q, Xia H. Preparation of cassava starch-gelatin yolk-shell microspheres by water-in-water emulsion method. *Carbohydrate Polymers*. 2023:121461.
18. Liu Z, Li H. Exploration of the exceptional capacitive deionization performance of CoMn2O4 microspheres electrode. *Energy & Environmental Materials*. 2023;6(1): e12255.
19. Othman AM, Elsayed AA, Sabry YM, Khalil D, Bourouina T. Detection of Sub-20 µm Microplastic Particles by Attenuated Total Reflection Fourier Transform Infrared Spectroscopy and Comparison with Raman Spectroscopy. *ACS omega*. 2023; 8(11):10335-41.
20. Hameed AR, Majdoub H, Jabrail FH. Effects of Surface Morphology and Type of Cross-Linking of Chitosan-Pectin Microspheres on Their Degree of Swelling and Favipiravir Release Behavior. *Polymers*. 2023;15(15):3173.

21. Hardainiyan S, Kumar K, Nandy BC, Saxena R. Design, formulation and in vitro drug release from transdermal patches containing imipramine hydrochloride as model drug. *Int J Pharm Pharm Sci.* 2017; 9:220-5.
22. Nabai L, Ghahary A, Jackson J. Novel, Blended Polymeric Microspheres for the Controlled Release of Methotrexate: Characterization and In Vivo Antifibrotic Studies. *Bioengineering.* 2023;10(3): 298.

© 2023 Al-Gharsan; This is an Open Access article distributed under the terms of the Creative Commons Attribution License (<http://creativecommons.org/licenses/by/4.0>), which permits unrestricted use, distribution, and reproduction in any medium, provided the original work is properly cited.

Peer-review history:

The peer review history for this paper can be accessed here:

<https://www.sdiarticle5.com/review-history/107189>